THE PUBLISHING HOUSE
OF THE ROMANIAN ACADEMY

PROCEEDINGS OF THE ROMANIAN ACADEMY, Series A,
Special Issue/2018, pp. 243–248

OPTIMALITY TO FLOW AND DESIGN OF BRANCHING DUCTS

Vinicius R. PEPE[*], Luiz A. O. ROCHA[**], Antonio F. MIGUEL[***]

[*] Federal University of Rio Grande do Sul, Department of Mechanical Engineering, Porto Alegre, Brazil,
[**] University of Vale do Rio dos Sinos (UNISINOS), Mechanical Engineering Graduate Program, São Leopoldo, Brazil.
[***] University of Evora, Department of Physics and Institute of Earth Sciences (ICT), Evora, Portugal

Corresponding author: Luiz A. O. ROCHA, E-mail: luizor@unisinos.br

Abstract. Complex flow systems such as the vascular and respiratory trees are made of large and small ducts connected together. While the Hess–Murray law is supported by a number of empirical studies, it will not always hold. To account to this, extensions of this law were put forth by several authors. The numerical study presented in this paper explores the performance of branching systems of ducts in terms of total fluid flow resistance and distribution of shear stresses for both laminar Newtonian and non-Newtonian fluids. Deviations from and extensions to Hess–Murray law are comprehensively identified and discussed. New insights into the dynamics within the assembly of ducts are presented.

Key words: Tree flow networks, Dendritic networks, Optimal design, Newtonian and non-Newtonian fluids, Hess-Murray law, Power-law fluids, Numerical study, Constructal design.

1. INTRODUCTION

Tree-shaped flow networks have been the subject of numerous investigations owing to its importance in understanding the behaviour of natural systems, and for the design of manmade systems [1–4]. Blood vessels supply cellular tissues with cells, nutrients and oxygen, and remove waste products of cellular activity, through branching vascular networks [5]. The respiratory tree supplies oxygen necessary for tissue metabolism and removes the produced carbon dioxide [4, 6]. Tissues, which make up the respiratory zone of this tree, support a very large gas exchange surface between air and blood that is ventilated and perfused with blood. For fluid transport systems the best flow configuration, that connects a point-to-volume and vice-versa is a tree network with an arrangement of increasingly smaller descending vessels [1–4, 7]. Assuming a minimum energy expenditure for blood flow and blood volume, Murray [8, 9] states that the optimal branching is achieved when the cube of the diameter of a parent vessel equals the sum of the cubes of the diameters of the daughters (Hess-Murray law). This optimum way to connect large and small vessels together is only valid long as the walls of vessels are impermeable, and the flow is laminar, Newtonian, steady, incompressible and fully developed [5, 6]. This $2^{-1/3}$ rule is able to describe network of veins and arteries, the airways of conducting zone of the respiratory tract, etc., but the smallest vessels deviate and airways of respiratory zone of the lungs, deviate from this rule. There is evidence that turbulent flows require an optimally $2^{-3/7}$ rule [10, 11]. However, fluid flow in living organisms is essentially laminar and evidences suggest that the exposure to turbulent flows might pose some health risk [6].

Blood includes erythrocytes (red blood cells), leukocytes (white blood cells) and thrombocytes (platelets) in an aqueous solution (plasma). Its rheology is largely influenced by the behaviour of the erythrocytes, mainly due to high concentration [5, 12]. Blood vessels exhibit diameters from 3 μm to 3 cm, and studies considering this effect on bifurcating design would be needed. In larger vessels, the flow is pulsatile due to pumping characteristics induced by the heart. Experimental studies suggest that if vessels experiences high shear rates (higher than 100 s^{-1}), it is reasonable to consider blood flow as a Newtonian fluid [5, 12]. In small vessels distant from the heart, the flow may be approached as steady. At shear rates lower than 100 s^{-1}, blood displays shear-thinning behaviour since its viscosity decreases with increasing shear rate. A power-law fluid model is applied by Miguel [5] and Revellin *et al*. [13] to derive expressions for these vessels.

It is observed a significant decrease of apparent blood viscosity in ducts with diameters in the range of 50–500 μm (Fåhræus-Lindqvist effect) [12]. The reason behind this effect is the formation of a cell-free layer near the wall of the duct, which has a reduced local viscosity (the core of the duct has a higher local viscosity). Miguel [12] investigated how the optimal branching of parent to daughter vessels is affected by occurrence of Fåhræus-Lindqvist effect.

Although first derived from the principle of minimum work, Hess-Murray law can be also obtained in the light of the constructal law [1–3]. For minimum resistance under global size constraints of a Newtonian fluid under laminar flow, Bejan *et al*. [11] showed that both diameter and length of the offspring vessels can be predicted conform a $2^{-1/3}$ rule. Other studies used the constructal law to propose the rules of design for flows of non-Newtonian fluids through bifurcating vessels, and for porous-walled vessels were also predicted [5, 6]. These rules were reported to depend on fluid behaviour index and on wall permeability. It is important to note that, the rules of design obtained based both on principle of minimum work and on constructal law are based on one-dimensional (1D) and two-dimensional (2D) analytical approaches, and involve many assumptions and simplifications listed in [14]. This study aims to obtain new insights into the dynamics of Newtonian and non-Newtonian flows in bifurcating vessels. A three-dimensional (3D) numerical analysis is performed to study fluid flow through T-shaped structures. The results are compared with analytical expressions presented by Murray [8, 9], Bejan *et al*. [11], Miguel [5] and Revellin *et al*. [13]. We chart the similitudes and differences, to provide a comprehensive view of the flow process.

2. MATHEMATICAL FORMULATION

2.1. Constructal law of design and extremum principles of entropy production

The emergence of configuration, defined by the constructal law, requires that the entropy changes, rather than staying the same [1–4, 15]. Consider that the fluid flow, Q, raised to the power of n is proportional to the pressure difference, ΔP. The rate of entropy generated, S_g, at absolute temperature, T, is given by

$$\frac{\mathrm{d}S_g}{\mathrm{d}t} = \frac{Q^n \Delta P}{T}. \tag{1}$$

Here n is the power-law index ($n < 1$ fluid with shear-thinning properties, $n > 1$ fluid with shear-thickening properties, $n = 1$ Newtonian fluid). As $Q^n = R^{-1}\Delta P$, in terms of flow resistance R, Eq. (1) may be rewritten as

$$R = \frac{\Delta P^2}{\left(\mathrm{d}S_g / \mathrm{d}t\right)}, \quad \text{or} \quad R = \frac{T\left(\mathrm{d}S_g / \mathrm{d}t\right)}{Q^{2n}}. \tag{2}$$

Minimum R for a specified potential (ΔP = constant) means maximizing of the entropy generation rate, but minimum R for a constant current (Q = constant), means minimizing the entropy generation rate.

2.2. Problem description

Consider a symmetric T-shaped flow system composed by cylindrical ducts designed according to

$$\frac{D_2}{D_1} = a_D, \quad \text{and} \quad \frac{L_2}{L_1} = a_L, \tag{3}$$

where D is the diameter, L is the length, the subscripts 1 and 2 mean parent and daughter ducts, and the scale factors a_D and a_L may vary between 0.1 to 1.0. The geometric constraints are [11]

$$V_{total} = \frac{\pi}{4}\left(D_1^2 L_1 + 2D_2^2 L_2\right), \text{ and } \quad A_{planar} = 2L_1 L_2 = \text{const},$$

which means the total volume occupied by the ducts and the total space occupied by the planar assembly of ducts are fixed.

2.3. Governing equations

Consider a laminar, steady and incompressible flow. Continuity and the momentum equations are

$$\nabla \vec{v} = 0, \tag{5}$$

$$\varphi \vec{v}(\nabla \vec{v}) = (\nabla P) - (\nabla \vec{\tau}). \tag{6}$$

Here **v** is the velocity, φ is the density, **τ** is stress and

$$\tau_{ij} = \mu Z_{ij}, \tag{7}$$

$$\mu = k\gamma^{n-1} \exp\frac{T_0}{T}, \tag{8}$$

where Z is the rate of deformation tensor, μ is the viscosity, T_0 is the reference temperature, k is the consistency index, and n is the power-law index. The Reynolds number for power-law fluid flows is [15]

$$\mathrm{Re}_D = \frac{4^{4-3n}\phi\varphi^{2-n}}{\pi^{2-n}KD_1^{4-3n}\left(\frac{3n+1}{4n}\right)^n}, \tag{9}$$

where Re_{Dn} is the generalized Metzner-Reed Reynolds number.

2.4. Numerical procedure

The governing Eqs. 5–7 are solved using a finite volume method and employing the segregated method with implicit formulation. A constant mass flow rate and an outflow boundary condition are used at the inlet and at the outlet, respectively. No-slip boundary conditions are applied at walls. Relaxation factors for momentum and pressure were set to 0.70 and 0.30, respectively. The residual values of the governing Eqs. 5 and 6 were all set to 10^{-4} and 10^{-6}, respectively. Details can be found in [14].

3. RESULTS AND CONCLUSIONS

Here we present a comprehensive set of results for laminar flow (Re_{Dn}=100) and for power-law indices $n < 1$ (shear-thinning fluid) and $n = 1$ (Newtonian fluid). The numerical study was carried out using the following fluids with the following properties: n = 0.66: ρ = 1041 kg/m^3 and k = 0.2 Pa·s^n (tomato paste 5.8% solid); n = 0.776: ρ = 1060 kg/m^3 and $k = 1.47\times10^{-4}$ Pa·s^n (blood); n = 1: ρ = 1.1405 kg/m^3 and $\mu = 1.9043\times10^{-5}$ Pa·s (air), ρ = 998 kg/m^3, $\mu = 8.91\times10$–4 Pa·s (water), and ρ = 1259.9 kg/m^3, $\mu = 7.99\times10^{-1}$ Pa·s (glycerine).

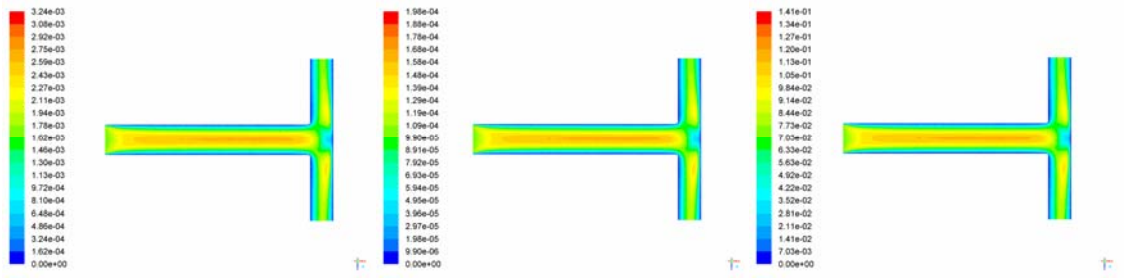

Fig. 1 – Velocity contours (middle plane) in a 3D T-structure ($D_2/D_1 = L_2/L_1 = 2^{-1/3}$): air, water and glycerine, respectively.

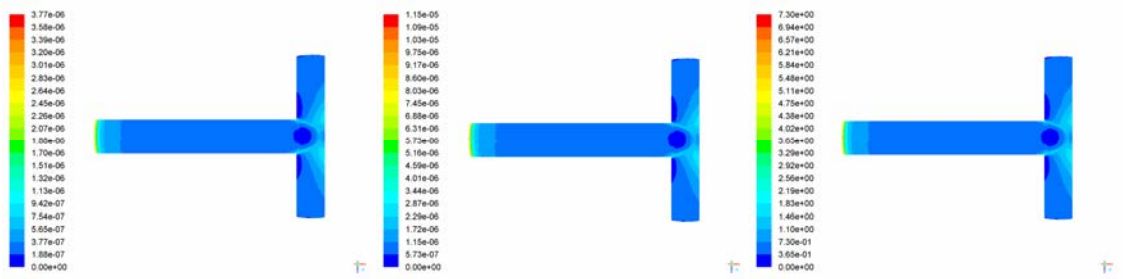

Fig. 2 – Shear stress contours (top plane) in a 3D T-structure ($D_2/D_1 = L_2/L_1 = 2^{-1/3}$): air, water and glycerine, respectively.

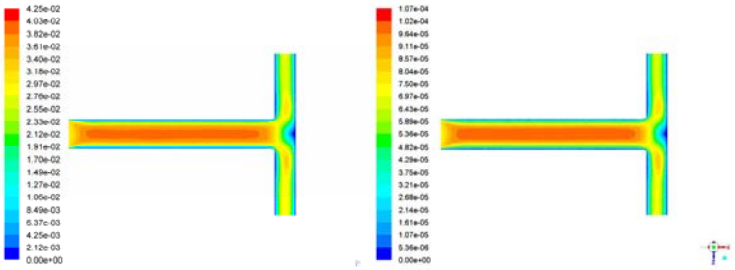

Fig. 3 – Velocity contours (middle plane) in a 3D T-structure ($D_2/D_1 = L_2/L_1 = 2^{-1/3}$): $n = 0.66$ (tomato paste 5.8% solid), $n = 0.776$ (blood), respectively.

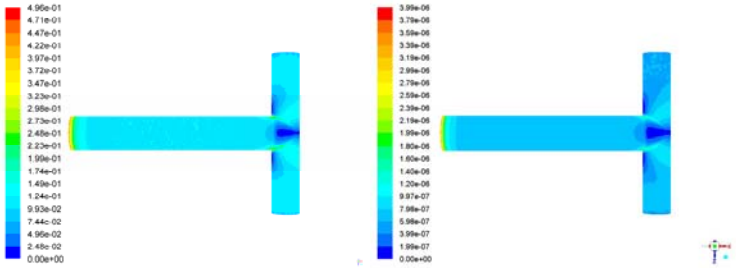

Fig. 4 – Shear stress contours (top plane) in a 3D T-structure ($D_2/D_1 = L_2/L_1 = 2^{-1/3}$): $n = 0.66$ (tomato paste 5.8% solid), $n = 0.776$ (blood), respectively.

Figures 1 and 2 show the velocity and shear stress contours for the Newtonian fluids. Although air, water and glycerine have different properties, the velocity and the shear stress profiles are similar. It is interesting to note that, although the geometry of the bifurcation is symmetric, velocity and shear stress are slightly asymmetric. This agrees with the findings of Andrade Jr *et al.* [16], and Pepe *et al.* [14] that also reported asymmetric velocities profiles. It has also been found a dependence of velocity asymmetric on Reynolds number [14]. As for Newtonian fluids, shear-thinning flows also show asymmetric velocity and shear stress distributions (Figs. 3 and 4). This means that these asymmetric distributions in symmetric geometries are common fingerprints to both shear-thinning and Newtonian fluids.

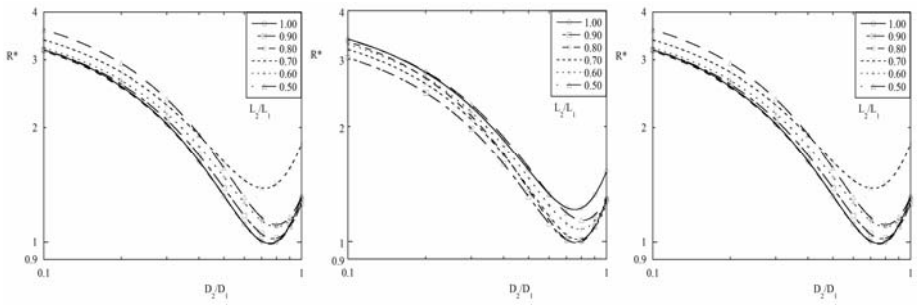

Fig. 5 – Dimensionless total flow resistance, R^*, of a *T*-flow structure ($n = 1$): air, water and glycerine, respectively.

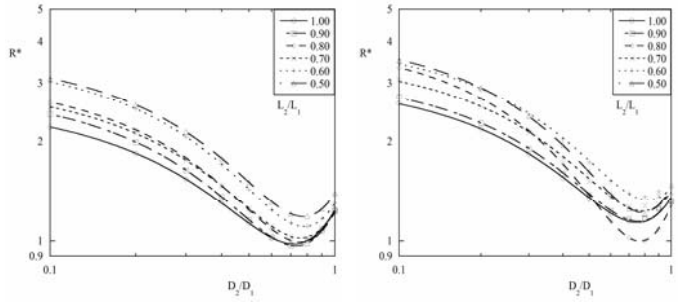

Fig. 6 – Dimensionless total flow resistance, R^*, of a *T*-flow structure: $n = 0.66$ (tomato paste 5.8% solid), $n = 0.776$ (blood), respectively.

According to Eq. 2, minimizing the entropy generation rate means minimizing the flow resistance under a constant fluid flow. Figures 5 and 6 show the total dimensionless flow resistance, R^*, for flows of Newtonian and shear-thinning fluids through T-shaped structures. The dimensionless resistance R^* is defined by the ratio of total flow resistance to the total flow resistance in a T-shaped assembly of ducts designed according to $D_2/D_1 = L_2/L_1 = 2^{-1/3}$. The scale factors a_D and a_L that allows a T-configuration with a minimum system-resistance are obtained and compared with those predicted analytically by [5] and [13] (Table 1). For Newtonian fluids the optimal a_D and a_L is independent of fluid properties. This may be explained by the similar velocity and shear stress contours depicted in Figs. 1 and 2. For shear-thinning fluid, the optimal scale factors a_D and a_L depend on power-law index n. These numerical results agree very well with the prediction of analytical models presented by [5, 8, 11, 13]. In an attempt to provide additional information, we also calculated the total flow resistance for each optimal T-shaped configuration (Table 2).

Table 1

Optimal branching scale factor for minimum flow resistance of a T-shaped assembly of ducts

power-law index n		Optimal assembly of ducts based on Figs. 5 and 6		Optimal assembly of ducts based on the analytical model of references [5, 8, 11, 13]	
		a_D	a_L	a_D	a_L
0.660	*(tomato concentrate)*	0.76	0.87	0.76	0.87
0.776	*(Blood)*	0.77	0.83	0.77	0.84
1.000	*(air water glycerine)*	0.79	0.79	0.79	0.79

Table 2

Flow resistance in each duct of an optimal T-shaped assembly of ducts

Total Flow Resistance ($Pa.s^n/kg^n$)	Power-law index n		
	0.660 *(tomato paste)*	0.776 *(blood)*	1.000 *(water)*
	$a_D = 0.76$, $a_L = 0.87$	$a_D = 0.77$, $a_L = 0.83$	$a_D = 0.79$, $a_L = 0.79$
Parent duct	2.36E-01	4.65E-04	4.26E-04
Daughter duct 1	7.25E-02	1.48E-04	1.62E-04
Daughter duct 2	7.35E-02	1.49E-04	1.63E-04
Junction parent-daughter ducts	4.70E-02	6.86E-05	1.72E-04
Total	3.32E-01	6.48E-04	6.75E-04

Table 2 shows that the flow resistance at parent duct is higher than in any other duct. It is remarkable to notice that the flow resistance in each daughter duct is not the same. This may be a direct consequence of the heterogeneous velocity and shear stress distributions shown at Figs. 1 to 4. It is remarkable to notice that the flow resistance at the junction of parent-daughter ducts is of same order of magnitude than the flow resistance at each daughter duct, exception for $n = 0.776$. This means that the flow resistance at the junction between parent and daughter ducts is not small enough to be negligible. In fact, Wechsatol *et al.* [17] suggested that the junction losses have a sizeable effect on optimized geometry when the svelteness factor defined by the ratio of the external to the internal length scales is lower than the square root of 10 (~3.2). In our study, the svelteness factor of T-configurations varies between 2.108 and 2.236. Notice that the

analytical models in the literature (see for example [6–11, 13]) assume that the flow resistance at parent-daughter junction is negligible, but even so they predict very well the optimal scale factor a_D and a_L.

To obtain further insights into the results depicted in Table 2, it is quite intuitive to consider the fluid flow like the flow of electric charges (electric current). For any system (fluid or electric charges), the total flowrate must be the same (principle of continuity). In our flow system, we assume that parent duct and the duct that connects parent-daughter ducts are resistors connected in series, and the daughter ducts are resistors connected in parallel. The total equivalent resistance of the resistors is

$$R_t \sim R_p + R_c + \frac{R_{d1} R_{d2}}{R_{d1} + R_{d2}}, \tag{10}$$

where R is the resistance and the subscripts t, p, c, d_1 and d_2 mean total equivalent, parent duct, junction parent-daughter ducts, d_1 daughter duct 1 and d_2 daughter duct 2, respectively. Eq. 10 reproduces rather well the numerical results depicted in Table 2, which means that is a good assumption to consider the parent duct and the junction of parent-daughter ducts as flow resistances connected in series. It is also important to note that the contribution of the flow resistances of daughter ducts to R_t is less than the smallest of the daughter resistances.

ACKNOWLEDGEMENTS

L.A.O. Rocha work is supported by CNPq, Brasília, DF, Brazil. A.F. Miguel acknowledge the funding provided by ICT, under contract with FCT (the Portuguese Science and Technology Foundation), Pest/OE/CTE/UI0078/2014.

REFERENCES

1. BEJAN, A., *Shape and Structure, from Engineering to Nature*, Cambridge University Press Cambridge, 2000
2. BEJAN, A., LORENTE, S., *Design with Constructal Theory*, Wiley, New Jersey, 2008.
3. BEJAN, A., *Evolution in thermodynamics*, Applied Physics Reviews, **4**, 011305, 2017.
4. MIGUEL, A.F., *Penetration of inhaled aerosols in the bronchial tree*, Medical Engineering and Physics, **44**, pp. 25–31, 2017.
5. MIGUEL, A.F., *Toward an optimal design principle in symmetric and asymmetric tree flow networks*, J. Theor. Biol., **389**, pp. 101–109, 2016.
6. MIGUEL, A.F., *Fluid flow in a porous tree-shaped network: Optimal design and extension of Hess–Murray's law*, Physica A, **423**, pp. 61–71, 2015.
7. MIGUEL, A.F., *Quantitative unifying theory of natural design of flow systems: emergence and evolution*, *Constructal Law and the Unifying Principle of Design*, Springer, 2013, pp. 21–38.
8. MURRAY, C.D., *The physiological principle of minimum work: I. The vascular system and the cost of blood volume*, Proceedings of the National Academy of Sciences of the United States of America, **12**, pp. 207–214, 1926.
9. MURRAY, C.D., *The physiological principle of minimum work applied to the angle of branching of arteries*, J. Gen. Physiol., **9**, pp. 835–841, 1926.
10. UYLINGS, H.B.M., *Optimization of diameters and bifurcation angles in lung and vascular tree structures*, Bull. Math. Biol., **39**, pp. 509–520, 1977.
11. BEJAN, A., ROCHA, L.A.O., LORENTE, S., *Thermodynamic optimization of geometry: T and Y-shaped constructs of fluid streams*, Int. J. Therm. Sci., **39**, pp. 949–960, 2000.
12. MIGUEL, A.F., Scaling laws and thermodynamic analysis for vascular branching of microvessels, Int. J. Fluid Mech. Res., **43**, pp. 390–403, 2016.
13. REVELLIN, R., ROUSSET, F., BAUD, D., BONJOUR, J., *Extension of Murray's law using a non-Newtonian model of blood flow*, Theor. Biol. Med. Model, **6**, *7*, 2009.
14. PEPE, V.R., ROCHA, L.A. O., MIGUEL, A. F., *Optimal branching structure of fluidic networks with permeable walls*, BioMed Research International, 5284816, 2017.
15. MIGUEL, A.F., *A study of entropy generation in tree-shaped flow structures*, Int. J. Heat Mass Trans., **92**, pp. 349–359, 2016.
16. ANDRADE Jr., J.S., ALENCAR, A.M., ALMEIDA, M.P., MENDES FILHO, J., BULDYREV, S.V., ZAPPERI, S., STANLEY, H.E., SUKI, B., *Asymmetric flow in symmetric branched structures*, Phys. Rev. Let., **81**, p. 926, 1998.
17. WECHSATOL, W., LORENTE, S., BEJAN, A., *Tree-shaped flow structures with local junction losses*, Int. J. Heat Mass Trans., **49**, pp. 2957–2964, 2006.